Journal of Photochemistry, 29 (1985) 217 - 225

ARTIFICIAL PHOTOSYNTHESIS: LIPOSOME CHARGE SEPARATION AIDED BY PHASE TRANSFER OF ELECTRON CARRIER*

I. TABUSHI, M. KINNAIRD and S.-I. KUGIMIYA
Kyoto University, Kyoto Yoshida (Japan)

Summary

Electron transporting membranes were used to improve the efficiency of charge separation in photoconversion systems. Multiphase systems were investigated using a liposomal membrane with a viologen electron relay/primary electron acceptor and flavine mononucleotide as the ultimate electron acceptor. A theoretical approach based on the concept of vectorial electron flow is described. This can be applied to the optimization of carrier-based photoconversion systems once the relevant kinetics parameters have become available. Attempts were made to improve the quantum yield of initial charge separation from the radical ion pair using an unsymmetrically metallated porphyrin dimer.

Much of the work performed in this laboratory in the field of solar energy research is modelled on bacterial photosynthesis; some aspects of bacterial photosynthesis have been used as an idealogical starting point for the development of artificial systems. Two entirely different aspects seem to be important in performing these model studies. Firstly, we may gain further insight into the mechanism and significance of natural bacterial photosynthesis (basic photochemistry, basic physical chemistry, catalysis etc.), maybe in a somewhat generalized way. Secondly, we can prepare an extremely efficient and reasonably practical photoconversion system which actually converts photoenergy to chemical energy.

It is best to base the construction of an artificial photosynthesis system on the fundamental processes that occur in natural photosynthesis: (i) photon absorption, (ii) energy transfer, (iii) charge separation, (iv) electron transport and (v) oxidative and reductive electron transport chain end reactions. We have been working towards the preparation of appropriate artificial molecular systems that promote these events.

Our group sees the following as some of the main problems that should be dealt with by any viable photoconversion system. (i) The back reaction from the initially charge-separated pair is highly favourable thermodynamically and, in most cases, also kinetically. This can drastically lower the

*Paper presented at the Fifth International Conference on Photochemical Conversion and Storage of Solar Energy, Osaka, Japan, August 26 - 31, 1984.

0047-2670/85/$3.30

overall quantum efficiency of any photoconversion system. (ii) The reductive and oxidative transport chain end products as well as many transporting intermediates are all highly energetic species, and thus can potentially react with each other to destroy the charge separation. (iii) Most systems proposed to date use some sacrificial electron donors and/or acceptors. Often these donors and/or acceptors are more expensive than the fuel they are used to produce and cannot be easily regenerated. This of course limits the practical use of such systems.

For the improvement of the charge separation efficiency, it is best to transfer one of the charge separated species generated in a certain phase to a different phase. The detailed consideration of a possible kinetic treatment appears later in this article but our first successful attempt was made a long time ago. We prepared an artificial membrane modified with a hydrophobic porphyrin–Mn complex as an electron transporting membrane and the membrane was used to accelerate a vectorial electron transport from an aqueous ascorbate phase (phase I) to an aqueous sodium hypochlorite phase (phase III) across the membrane phase (phase II) [1]. After this initial success, we have been gradually developing this concept of vectorial electron flow. The second system we would like to discuss is shown in Fig. 1. It is a homogeneous system using a water soluble photocatalyst, zinc(tetrasodium sulphonate phenyl)porphyrin ($ZnT_{SO_3Na}PP$) as the primary electron donor. A modified methyl viologen derivative, *N*-hexyl-4,4′-bipyridinium dichloride is the electron carrier transporting electrons. The significant feature of the system is the appropriate oxidation–reduction potential of this viologen electron carrier [2]. A number of electron donors could be used, such as ascorbic acid, sodium thiosulphate etc. The ultimate electron acceptor is the proton, which is reduced to dihydrogen at colloidal platinum supported on polymers. This system is able to produce dihydrogen relatively efficiently, with a quantum yield for hydrogen production of around 10%. However, one of the main drawbacks of this system, besides the fact that it uses a sacrificial donor, is that the dehydroascorbic acid produced in the photoreaction will react with the viologen cation radical electron relay to produce viologen dication and ascorbic acid. We feel that this type of reaction is an inherent disadvantage of homogeneous systems.

After the successes with electron transport across the membrane, study shifted to multiphase systems. The third system which we discuss is shown in

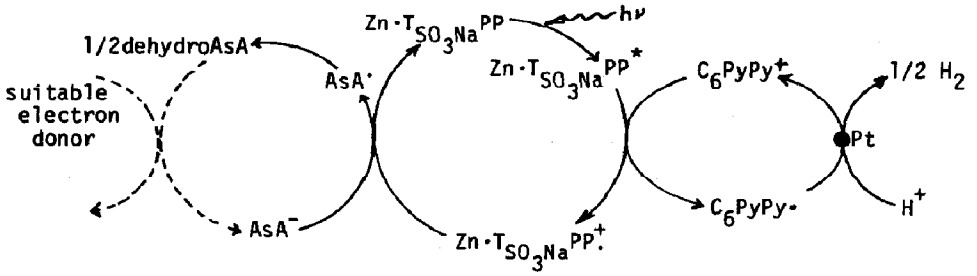

Fig. 1. Hydrogen production system.

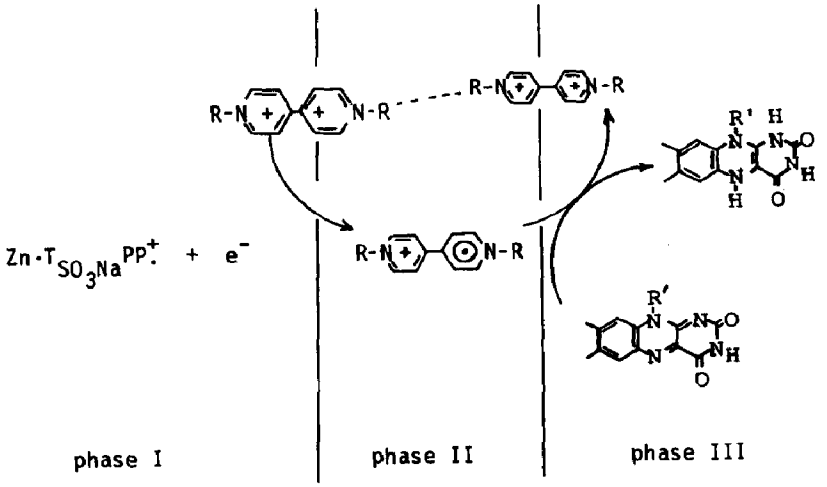

Fig. 2. Three-phase system for photoproduction of FMNH.

Fig. 2; it is a prototypical three-phase system. The photocatalyst is the same as in the first system (*i.e.* $ZnT_{SO_3Na}PP$). The electron relay/acceptor is another modified viologen, this time a hexyl viologen, *N*,*N*′-dihexyl-4,4′-bipyridinium dichloride. The ultimate electron acceptor in this case is flavine mononucleotide (FMN). The ultimate electron donor used in this system is sodium thiosulphate, which is known to be one of the major electron sources in bacterial photosynthesis. The phase transfer of viologen cation radical from the aqueous phase I into the aqueous phase III is activated by the addition of a surfactant cetyltrimethylammonium bromide (CTAB) and stirring is necessary [3]. This shows that phase transfer is crucial to the functioning of the photosystem. This photosystem is also capable of generating the reduced accept dihydroflavin mononucleotide (FMNH) with a quantum yield of about 10%, but the limiting factor is the small non-aqueous phase surface area to volume ratio.

For this reason, attention has turned to liposomal systems, which have very large hydrophobic phase surface area to volume ratios. The system at present being studied is shown in Fig. 3. The photocatalyst is again $ZnT_{SO_3Na}PP$ and the ultimate electron acceptor is again FMN, which has structure and function very similar to those of dihydronicotinamide adenine dinucleotide (NADH), the main product in bacterial photosynthesis. However, the viologen electron relay/primary electron acceptor is now a symmetrical viologen. The length of the alkyl chains attached to the nitrogens is varied. The ultimate electron donor is sodium thiosulphate. Two configurations have been studied, one with the photocatalyst and electron source in the exterior aqueous phase and the electron acceptor in the interior aqueous phase, and vice versa. The results from both configurations are very similar, and we will limit discussion to the first. Irradiation of this system with visible light gives rise to a rapid production of FMNH in the interior aqueous phase, again with a quantum yield of

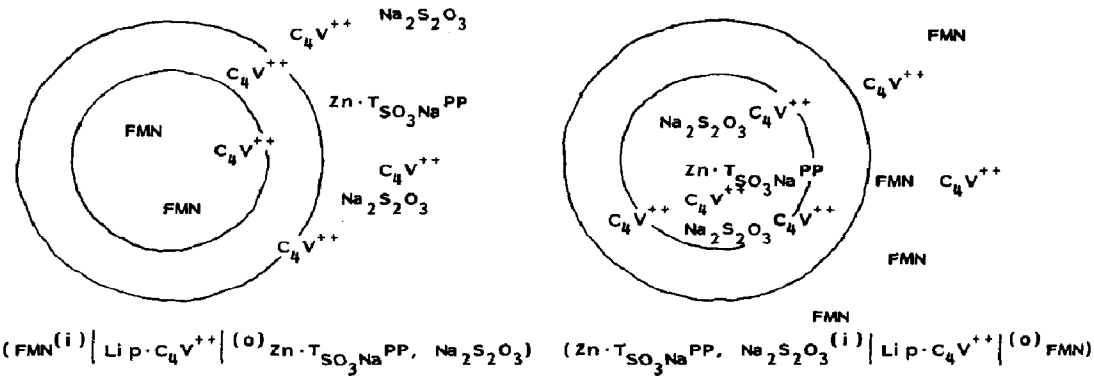

Fig. 3. Bacterial-type artificial photosynthesis cells.

around 10% under the best conditions. Both the rate and quantum yield of FMNH production are strongly dependent on the length of the alkyl chain attached to the viologen. Futhermore, the rate of electron transport in the dark, again mediated by viologens of various chain lengths, behaves the same. This and other independent experiments demonstrate that the rate of flux of viologen (at first cation radical, and later, viologen dication) through the liposomal membrane is the controlling kinetic factor in the overall efficiency and rate. Independent experiments have shown that neither the rate of quenching nor the rate of reduction of FMN by viologen cation radical is important in determining the overall rate or quantum yield of FMNH production.

In Fig. 4 the evolution of the viologen cation radical concentration in the system, followed spectrophotometrically at 605 nm, is shown. The initial rapid increase corresponds to the situation where V^{+} is rapidly entering the liposomal membrane after charge separation occurs. This reduces the efficiency of the diffusional back reaction and thus allows the rapid build-up of viologen cation radical in the system. This situation may be best interpreted by using the model shown in Fig. 5. A system having an excellent charge separation efficiency may be designed as Sutin pointed out [14]. This system, however, is even further improved by the introduction of another phase (or other phases) as shown in Fig. 6. The concentration of V^{+} mostly in the hydrophobic phase then begins to reach a plateau. This short-lived

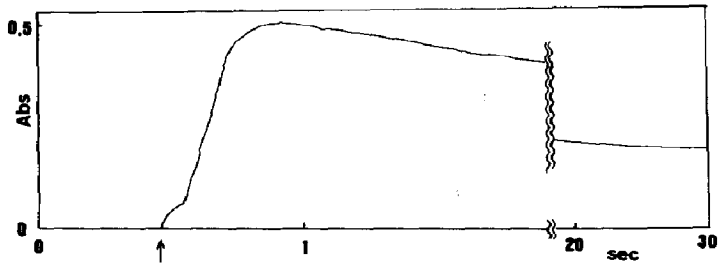

Fig. 4. The evolution of $[V^{+}]$ with time in the artificial photosynthesis cells (monitored at 605 nm).

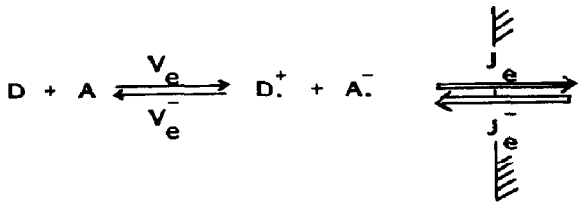

Fig. 5. Charge separation aided by interphasial flux.

plateau corresponds to the situation where the rate of production of $V^{+\cdot}$ in the exterior aqueous phase is balanced by the rates of flux of viologen through the liposomal membrane (J_o and J_i), and the rate of reaction of $V^{+\cdot}$ with FMN in the interior aqueous phase. After this plateau is reached, the concentration of viologen cation radical begins to decrease, owing to a relatively rapid reaction between viologen cation radical and FMN. Then V^{2+} is over-accumulated in the interior phase and a new flux of V^{2+} is generated. This latter situation is caused by a relatively slow rate of transport of viologen dication out of the interior of the liposome. Eventually this gives rise to a final steady state where all the fluxes involved are balanced.

We would now like to turn the discussion to a theoretical approach developed in this laboratory for the analysis of this system. The theoretical approach used here is also a general approach, and can be applied to many similar systems involving a phase transfer carrier mechanism. Use of this approach can readily allow quantification of such systems, where traditional kinetics approaches fail due to the complexity of the systems.

The first step is to state simply in mathematical terms the qualitative description of the liposomal photosystem. In a mathematical description, the flux of viologen cation radical across the liposomal membrane into the interior aqueous phase is exactly the same as the flux V_o of viologen cation radical into the system, caused by the reaction of viologen dication with excited $ZnT_{SO_3Na}PP$ photocatalyst. We call the latter reaction "flux generation", since the reaction gives rise to the flux of viologen cation radical into the system. Similarly, we can consider the reaction of viologen cation radical with FMN in the interior aqueous phase to be a flux V_i of viologen cation radical out of the system. Since this reaction acts as a "sink" for viologen cation radical, we can call this reaction "flux convergence". The flux of viologen cation radical across the membrane into the interior aqueous phase is easy to conceive of as a flux J_c. It is a physical flux of a species through a

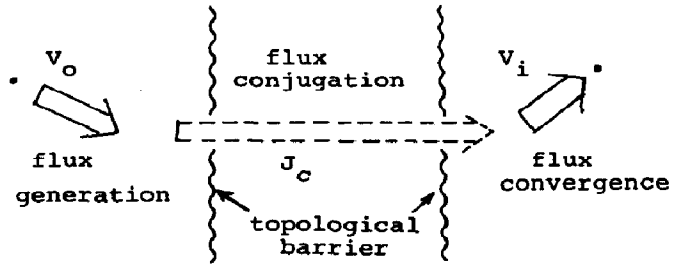

Fig. 6. Flux conjugation by vertical flux interaction.

surface. As Fig. 6 shows, this flux has a special relationship with the two fluxes v_o and v_i. Clearly, the rate of flux of viologen cation radical into the interior aqueous phase is a function of the rate of flux of viologen cation radical into the system, $J_c = f(v_o)$. Also, clearly, the rate of flux of viologen cation radical out of the system is related to the rate of flux of viologen cation radical through the liposomal membrane, $v_i = f'(J_c)$. These fluxes are directly interacting. It follows from the above relationships that there must therefore be an indirect interaction between the fluxes v_o and v_i, $v_o = g(v_i)$. Intuitively this makes sense. The rate of reaction between FMN and viologen cation radical in the interior aqueous phase must be related to the rate of production of viologen cation radical in the exterior aqueous phase. Therefore, we call the flux J_c a "conjugating" flux, by analogy with systems of conjugated C=C bonds, where the last carbon in a chain is influenced by the first, and vice versa. The interaction of fluxes in this manner is called "flux conjugation". This type of flux interaction is called "vertical", because, with respect to a plane drawn normal to the first flux v_o, all the subsequently conjugated fluxes are also normal to this plane.

This present flux interaction is different from coupling obtained by the use of the Onsager equation where the flux interaction $J_1 = f(J_2)$, [5 - 7]. The flux equations discussed above can be related to measurable quantities, such as reaction rates, surface areas, concentrations etc. By using these relationships, and the pseudo-steady-state relationship (1), or the true steady state relationship (2), then useful unknown quantities can be calculated.

$$v_o^{+\cdot} = J_o^{+\cdot} = J_i^{+\cdot} = v_i^{+\cdot} \tag{1}$$

$$v_o^{+\cdot} = J_o^{+\cdot} = J_i^{+\cdot} = v_i^{+\cdot} = v_o^{2+} = J_o^{2+} = J_i^{2+} = v_i^{2+} \tag{2}$$

The pseudo-steady state equation describes mathematically what was described quantitatively before. A similar situation holds for the steady state equation. In this case, all of the fluxes involving a V^{2+} are the analogous fluxes of viologen dication into the system in the interior aqueous phase, through the liposomal membrane and out of the system in the exterior aqueous phase.

By the use of the pseudo-steady-state equation, the concentrations of viologen cation radical in all three phases can be calculated. By a normal kinetics analysis, this would be most difficult. The results of this calculation are given in Table 1. From this table, we can see that there is still a driving force for the entry of viologen cation radical into the liposomal membrane in the pseudo-steady-state. We can also see that the driving force for the entry of viologen into the interior aqueous phase is quite large.

As is often the case, the experimental optimization of the chain length of the viologen carrier came before the development of the mathematical approach. However, another potential use of the approach described here is the easy optimization of a carrier-based photoconversion system, based on the optimization of the pseudo-steady-state and true steady state equations. For this process, it is necessary to know *a priori* most of the kinetics parameters involved, as well as the surface area of the liposomes used as a barrier

TABLE 1

	Short-lived steady state	*Equilibrated state*
$\frac{[V^{+\cdot}]_o}{[V^{+\cdot}]_m}$	0.10	1.47×10^{-3}
$\frac{[V^{+\cdot}]_m}{[V^{+\cdot}]_i}$	680	680

$[V^{+\cdot}]_m$, viologen cation radical concentration in the membrane.

and the volume of the system. However, these kinetics parameters can often be measured by independent experiments on subsystems of the whole system. With these parameters available, it merely becomes a mathematical exercise to optimize such a system. Flux optimization can be accomplished by modifying such parameters as reaction velocity, hydrophobicity/hydrophilicity balance, surface area-to-volume ratios etc. We feel that this is the true power of this approach to the analysis of systems. Although at the present moment, we do not have enough of the kinetics parameters to readily perform such an optimization, experimentation along these lines is now under way.

The above discussion pertains to optimization of the photoconversion system in terms of post-quenching events. The 10% quantum yield of FMNH production is respectable (see Table 2) but could be improved. The use of a multiphase system and the added electron source are to a large extent capable of suppressing the diffusional back reaction, but do not increase the quantum yield of initial charge separation from the radical ion pair. The

TABLE 2

Production of flavin mononucleotide

	Chemical yield[a] (%)	*Quantum yield* (%)	*Observed recycling numbers*	
			$ZnT_{SO_3Na}PP$	C_4V^{2+}
A	95	10	$120(10^4)$[b]	$30(10^2)$[b]
B	95	3	$2.5(30)$[b]	$1.4(10^2)$[b]
C		3.8×10^{-2} [c]	ref. 8	
D		0.44[c]	ref. 9	
E		2.4[c]	ref. 10	

A: ($ZnT_{SO_3Na}PP$, $Na_2S_2O_3$ $^{(i)}|Lip \cdot C_4V^{2+}|^{(o)}$ FMN); B: (FMN $^{(i)}|Lip \cdot C_4V^{2+}|^{(o)}$ $ZnT_{SO_3Na}PP$, $Na_2S_2O_3$); C: (edta $^{(i)}|Lip \cdot Ru^{2+}(bpy)_3|^{(o)}$ C_7V^{2+}, Zn^{2+}); D: (edta, K^+ $^{(i)}|Lip \cdot Ru^{2+}(bpy)_3|^{(o)}$ C_7V^{2+}, K^+); E: (MeV^{2+} $^{(i)}|Lip|^{(o)}$ $Ru^{2+}(bpy)_3$, edta). (Lip ≡ lipsome.)

In the above C_nV^{2+} is a viologen having n $-C_n$ chains.

[a] Based on FMN used.

[b] This work, based on catalysts consumed.

[c] Quantum yield of viologen cation radicals.

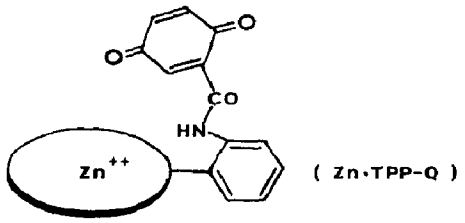

Fig. 7. A covalently linked donor–acceptor pair.

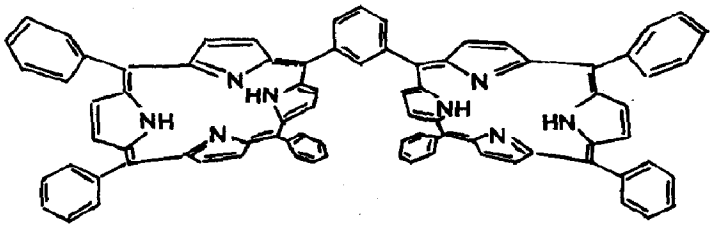

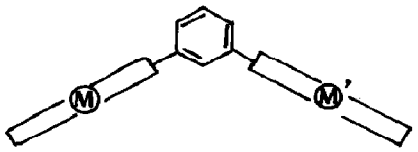

COMPOUND	M	M'
Gable	H_2	H_2
Zn_1Gable	H_2	Zn^{2+}
Zn_2Gable	Zn^{2+}	Zn^{2+}

Fig. 8. Gable porphyrin and some metal complexes of gable porphyrin.

remainder of the discussion will be devoted to attempts to improve the quantum yield of separated radical ions.

The first attempt in this laboratory in this area was to synthesize a metalloporphyrin–quinone pair as a first member of this often-employed family [11] where the donor was covalently linked to the acceptor (see) Fig. 7). This naive approach was rewarded by the photoproduction of the quinone anion radical–porphyrin radical charge separated pair in reasonable quantum yield. An electron spin resonance signal was observed that could be attributed to the porphyrin cation radical–quinone anion radical pair. However, this charge separated state is not long lived as expected.

The system now under study consists of an unsymmetrically metallated porphyrin dimer (see Fig. 8). The monometallated compound Zn_1gable shares some aspects in common with bacterial reaction centres. Thus we were interested in studying the photochemistry of a series of related porphyrins. The synthesis of the monozinc gable will be described in a subsequent paper. The absorption characteristics of a series of porphyrins of interest are summarized in Table 3. From this table, it is clear that the interaction of the two porphyrin rings in the case of gable porphyrins is not very large (Soret splitting for example). Thus ground state interactions are moderate.

From the fluorescence measurements of a series of porphyrins of interest, we can see that there is almost no emission from the ZnP part of the

TABLE 3

Visible absorption spectral properties of H_4gable, Zn_2gable and Zn_2gable

Species	*Soret* (log ϵ)	*Q band* (log ϵ)
H_4gable	416(5.69) 428(5.68)	515(4.54) 552(4.16) 592(4.04) 648(3.94)
Zn_1gable[a]	415(5.69) 429(5.68)	515(4.33) 551(4.44) 593(4.03) 647(3.61)
Zn_1gable[b]		515(4.30) 551(4.45) 594(4.02) 648(3.64)
Zn_2gable	416(5.74) 431(5.69)	552(4.57) 594(4.01)

All spectra were taken in ethanol-free chloroform at 24 ± 1 °C.
[a]Measured spectrum.
[b]Theoretical spectrum calculated from assuming $\epsilon_{Zn_1gable} = \frac{1}{2}(\epsilon_{Zn_2gable} + \epsilon_{H_4gable})$.

porphyrin. This result is almost into the 550 nm band, which is 67% zinc porphyrin(ZnP) in nature. Thus the quantum yield of free base emission is independent of which porphyrin is excited. This indicates that energy transfer from the excited singlet ZnP is efficient, and that once the energy of excitation is transferred, for some reason it is not re-transferred back to the ZnP. A study is now under way to determine the triplet photochemistry of Zn_1gable. What is clear from the data obtained so far is that the interaction of the two porphyrin rings in gable and its derivatives are much greater in the excited state than the ground state and these dimeric porphyrin derivatives seem to show promise for the future construction and analysis of artificial photosystem models.

References

1 I. Tabushi and M. Funakura, *J. Am. Chem. Soc.*, *98* (1976) 4684.
2 I. Tabushi and A. Yazaki, *J. Org. Chem.*, *46* (1981) 1899.
3 I. Tabushi, N. Koga and K. Iwasaki, *Tetrahedron Lett.*, (1980) 373.
4 C.-Y. Mok, A. W. Zanella, C. Creute and N. Sutin, *Inorg. Chem.*, *23* (1984) 2891.
5 I. Tabushi and T. Nishiya, *J. Am. Chem. Soc.*, *103* (1981) 6963.
I. Tabushi and T. Nishiya, *Tetrahedron Lett.*, (1982) 2661.
6 I. Tabushi and T. Nishiya, *Tetrahedron Lett.*, (1981) 4989.
7 I. Tabushi, T. Nishiya, M. Shimomura, T. Kunitake, H. Inokuchi and T. Yagi, *J. Am. Chem. Soc.*, *106* (1984) 219.
8 W. E. Ford, J. W. Otvos and M. Calvin, *Proc. Nat. Acad. Sci.*, *76* (1979) 3590.
9 C. Laane, J. W. Otvos, W. E. Ford and M. Calvin, *Proc. Nat. Acad. Sci.*, *78* (1981) 2017.
10 M. S. Tunuli and J. H. Fender, *J. Am. Chem. Soc.*, *103* (1981) 2507.
11 I. Tabushi, N. Koga and M. Yanagida, *Tetahedron Lett.*, (1979) 257.